

# Control of dual isoforms of Ca<sup>2+</sup> release channels in muscle

EDUARDO RÍOS and JINGSONG ZHOU

Section of Cellular Signaling, Department of Molecular Biophysics and Physiology,  
Rush University, Chicago, IL, USA

## ABSTRACT

Here we compare excitation-contraction coupling in single muscle cells of frogs and rats. Because amphibians have isoform 3 (or  $\beta$ ) of the ryanodine receptor/Ca<sup>2+</sup> release channel, in addition to 1 ( $\alpha$ ), which is also present in the mammal, any extra feature present in the frog may in principle be attributed to isoform 3. Ca<sup>2+</sup> release under voltage clamp depolarization has a peak and a steady phase in both taxonomic classes, but the peak is more marked in the frog, where the ratio of amplitudes of the two phases is voltage-dependent. This dependence is a hallmark of CICR. Confocal imaging identified Ca<sup>2+</sup> sparks in the frog, but not in the voltage-clamped rat cells. Because Ca<sup>2+</sup> sparks involve CICR both observations indicate that the contribution of CICR is minor or null in the mammal. The “couplon” model well accounts for observations in the frog, but assumes a structure that we now know to be valid only for the rat. A revised model is proposed, whereby the isoform 3 channels, located parajunctionally, are activated by CICR and contribute its characteristic global and local features. Several issues regarding the roles of different channels remain open to further study.

**Key words:** Excitation-contraction coupling, sarcoplasmic reticulum, Ca<sup>2+</sup> sparks, ryanodine receptor, calcium-induced calcium release.

## INTRODUCTION

As an intracellular messenger, Ca<sup>2+</sup> participates in a wide range of processes. In muscle, action potentials in the plasma membrane and transverse (T) tubules cause Ca<sup>2+</sup> channels of the sarcoplasmic reticulum (SR) to open. The ensuing Ca<sup>2+</sup> release initiates contraction (e.g. Cheung, 2002). In this article we will summarize studies that explore the differences between amphibian and mammalian muscles in regard to this excitation-contraction (EC) coupling function.

## STRUCTURAL AND FUNCTIONAL DIFFERENCES BETWEEN AMPHIBIAN AND MAMMALIAN MUSCLE

Major differences in the molecular makeup of fast twitch muscles of frogs and mammals have long been known. First, the binding

assays for dihydropyridines and ryanodine consistently yielded a lower DHPR/RyR for frogs, as if they had extra release channels. The early biochemical literature was reviewed by Shirokova et al. (1996). These authors took advantage of techniques developed by Delbono and Stefani (1993) and García and Schneider (1995) to carry out direct comparisons of Ca<sup>2+</sup> release between frogs and mammals. A difference in the isoform complement of ryanodine receptors later became known, whereby the frog fast muscles contain RyR1 or  $\alpha$ , and RyR3, or  $\beta$ , in approximately equal densities (rev. by Sutko and Airey, 1996; Ogawa et al., 1999), while in most muscles of adult mammals the isoform 1 is found exclusively (Marks et al., 1989; Takeshima et al., 1989; Flucher et al., 1999). Finally, Felder and Franzini-Armstrong (2002) reported an association between the presence of RyR3 and extra channels, which in triadic cross sections

appear as feet-like structures in a parajunctional position. These parajunctional channels are arranged in double or triple rows, but in glancing, sections appear to constitute a lattice geometrically different than that of the junctional double row. Therefore, the authors concluded that parajunctional arrays were composed of a different isoform, namely RyR3.

It is reasonable to expect a functional correlate of these structural differences. We have used this expectation as a guide for experiments and interpretation. The specific hypothesis is that the function of EC coupling will be richer and more complex in the amphibian. A logical consequence is that any distinct functional features present in the frog but not the mammal will be assigned to the RyR3, alone or in interaction with the other isoform, while common features will be taken as directly produced at or by the RyR1 channels.

#### FUNCTIONAL DIFFERENCES WERE FIRST UNVEILED AT THE WHOLE CELL LEVEL

We started this approach with N. Shirokova et al. (1996), using a "global" technique in which  $[Ca^{2+}](t)$  and release flux were derived from photometric signals of fluo-3 or antipyrylazo III in voltage-clamped fibers from frogs or rats. An intriguing difference was found in the kinetics of the  $Ca^{2+}$  transient elicited by pulse depolarization, which had a clear early peak in the frog, but in the rat only a fast rise to an approximately steady level (or sometimes a dull peak). This in turn resulted in a release flux (calculated by the methods of Melzer et al., 1987) with a much more marked and rapidly decaying peak in the frog.

The peak in turn had been interpreted before as a manifestation of the amplification by CICR of a directly voltage-operated  $Ca^{2+}$  flux (Ríos and Pizarro, 1988). In this view (Fig. 2), the release channels directly under voltage sensors open first and remain open for as long as the pulse lasts, while the channels without voltage sensors open rapidly by CICR, then close rapidly (presumably inhibited by the local increase in  $[Ca^{2+}]$  due

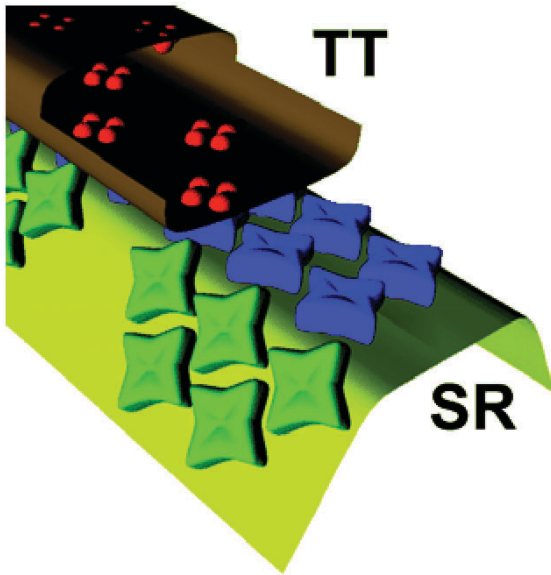
to channel opening). Accordingly, the ratio of the peak of the release waveform over its quasi-steady value was a measure of the "gain" contributed by CICR.

Figure 3 shows the voltage dependence of this gain (peak/steady ratio). The value is greater everywhere for the frog, and it is also voltage-dependent, going through a marked maximum at intermediate voltages (ca. -30 mV). This voltage dependence was explained quantitatively by Shirokova et al., (1996) using the model of Ríos and Pizarro (1988).

The explanation is in Figure 4, depicting a two-row array of channels with intercalated voltage- (V) and  $Ca^{2+}$ - (C) operated channels. Consider first the situation at very low voltage, when only one V channel is activated (for example, the one in black in the center of the top row). The thick central curves plot local  $[Ca^{2+}]$  near the open channel (*i.e.* Stern, 1992) and the horizontal line a threshold for activation of C channels by  $Ca^{2+}$ . The two neighboring C channels, marked with a \*, face a supra-threshold concentration, hence they open and contribute to the peak release at this voltage. The "gain" of CICR is (2 C channels) / (1 V channel), or 2.

Next, imagine the system at a somewhat higher voltage, with three V channels open (red). The two C channels flanking each open V channel will be opened under the influence of their "master" V channel acting alone or together. The other C channels in the same row will also open, but due to the summation of contributions to local  $[Ca^{2+}]$  ("sum", in thin trace). The gain therefore will be greater than 2. Obviously at greater voltage the number of V channels activated will still increase, while the number of C channels (at least for this row) has reached maximum. The gain can only go down.

The increasing-then-decreasing gain is thus shown to be a fundamental property of CICR, a hallmark in this structural scenario. Thus it was enlightening to see the next finding of Shirokova et al. (1996). As shown in Figure 3, the ratio peak/steady release flux in the rat was lower and devoid of the increase at intermediate voltages. This was interpreted as an indication of a



**Figure 1.** Two RyR isoforms form distinct arrays in non-mammals. From Felder and Franzini-Armstrong (2002).

lesser or perhaps null contribution of CICR to  $Ca^{2+}$  release in the mammal.

The lesser peak of  $Ca^{2+}$  release in the mammal makes teleologic sense. Indeed in mammals the transverse tubules and triadic junctions are closer to the functional target of the released  $Ca^{2+}$  –troponin C– in the areas of filament overlap. As suggested by Dr. Elizabeth Stephenson (cited by Shirokova et al., 1996) and independently proposed by Volpe and Simon (1991), this diffusional advantage should make it possible to produce the contractile signal without the high local flux of the frog and without the multi-ion coupling mechanisms needed to achieve it. A lower release flux would have many benefits, including faster

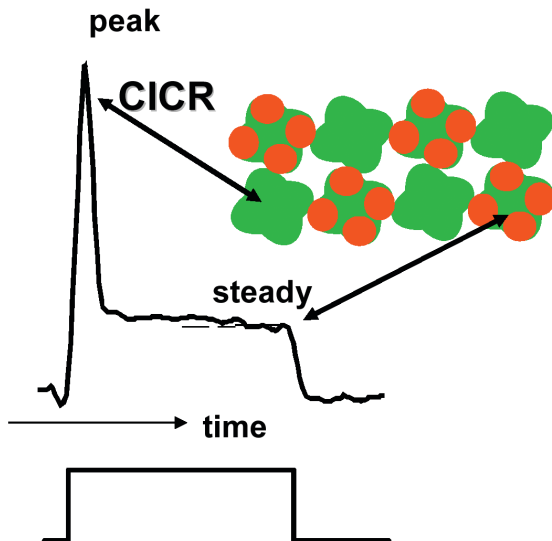


**Figure 2.** Flux through channels underlying voltage sensors is directly controlled by them and constitutes the steady component of the waveform, while the peak is due to the other channels, activated and then closed by  $Ca^{2+}$ . From Ríos and Pizarro (1988).

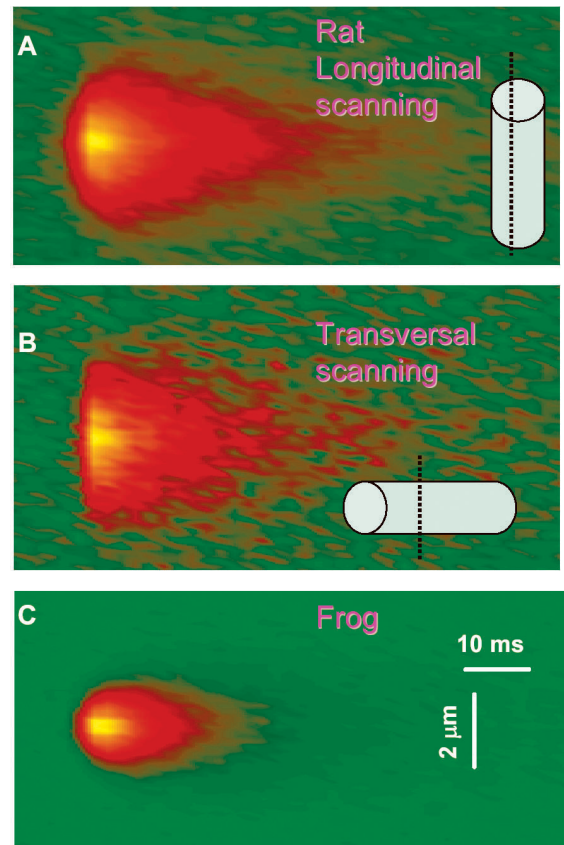


**Figure 6.** Averages of sparks detected in line scans parallel (A) or perpendicular to the fiber axis. Rat sparks (A, B) are wider than the frog's and wider in transversal scans (B). From Zhou et al. (2003).

rise and dissipation of  $[Ca^{2+}]$  near the physiologic target, improved stability of the release mechanism and a less demanding  $Ca^{2+}$  retrieval process.

#### MAJOR FUNCTIONAL DIFFERENCES AT THE LOCAL LEVEL

The study of EC coupling was drastically altered by the realization that most if not all of  $Ca^{2+}$  release takes the form of  $Ca^{2+}$  sparks (Cheng et al., 1993; Tsugorka et al., 1995; Klein et al., 1996, see also Schneider and Rodney, this issue). The defining property of sparks is their abrupt termination, after an open time that varies narrowly (around 5 ms) in skeletal muscle. This brevity is reminiscent of the kinetic peak of  $Ca^{2+}$  release visible in the cell-averaged records, the similarity being a strong indication that the peak of  $Ca^{2+}$  release (which is a good representation of physiological response upon an action potential) may be just the result of superposition of synchronized sparks. Hence, these results highlight the relevance of  $Ca^{2+}$  sparks and their study.

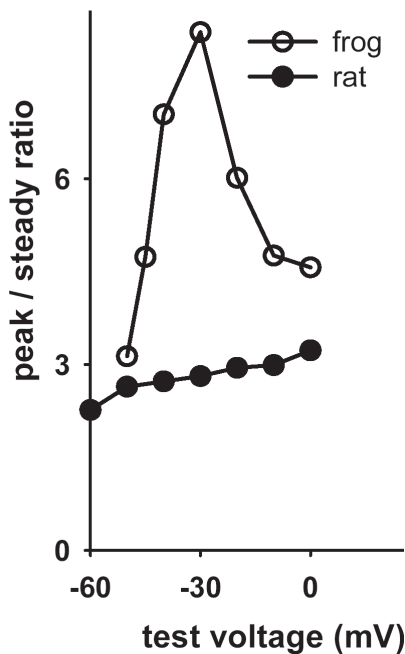


**Figure 3.** The ratio of amplitudes of the two phases of release flux has strikingly different voltage dependence in frog and rat. From Shirokova et al. (1996).

An eloquent presentation of this concept is found in a study of Klein et al. (1997), where it is demonstrated that the global (whole-cell-averaged)  $Ca$  release flux waveform  $R(t)$  could be approximated as a sum of release in sparks. This is mathematically expressed by

$$R(t) = \int_0^t L(u)E(t-u)du \quad (1)$$

where  $L(t)$  is the distribution of latencies of sparks (a function of latency  $t$  that also depends on pulse voltage), and  $E(t)$  is the time course of the elementary event of release, a pulse of constant current and duration equal to the average rise time of a spark in the study of Klein et al., (1997) This equality was shown to apply, but only qualitatively, yielding a function of time that is less peaky than the actual  $R(t)$ , especially at intermediate voltages. The implication is that release flux in frog muscle can be approximated by a superposition of sparks, but that the sparks studied in isolation (by resorting to low voltages or partial inactivation schemes) may be different than the events occurring in a fully activated cell under physiological stimulation.

Given this happy consensus on the significance of sparks, it was surprising that in mammalian muscle sparks were observed only under rather artificial conditions (Kirsch et al., 2001; Zhou et al., 2003; Szentesi et al., 2004). Sparks were not observed under voltage-clamp depolarization (Shirokova et al., 1999). This stimulus instead produced “embers” (González et al., 2000a), very different events that can also be observed occurring spontaneously (Kirsch et al., 2001; Zhou et al., 2003; Hollingworth et al., 2003) and are the consequence of openings of single RyR channels.

As in the study of Klein et al. (1997) one may reproduce qualitatively the waveform of  $Ca^{2+}$  release in the rat, by the convolution equation (1), using a constant current (commensurate with a single channel opening) as  $E(t)$  (Csernoch et al., 2004). Again, this procedure leads to a qualitatively adequate but less “peaky” kinetic waveform.

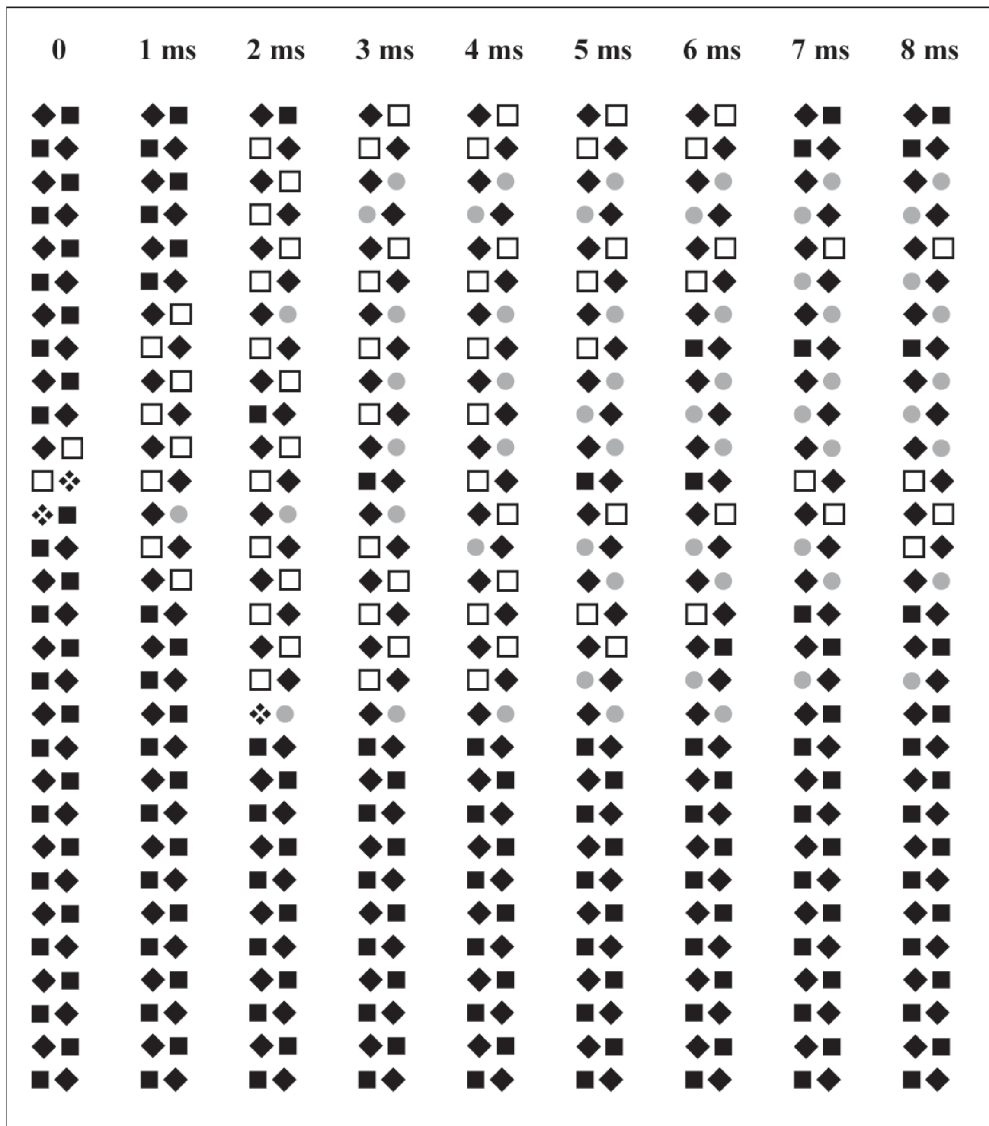


**Figure 5.** A series of “snapshots” of a 60 channel couplon at 1 ms intervals during a depolarization to -50 mV. A coincident opening of two neighboring *V* channels triggers *C* channel openings, which then propagate as a wave along the length of the couplon until stopped by random inactivation events. ◆=closed *V* channel, ■=closed *C* channel, ❖=open *V* channel, □=open *C* channel, ●=inactivated *C* channel. From Stern et al. (1997).

One may conclude that the basic reductionist program of accounting for global  $Ca^{2+}$  release by superposition of elementary events has now been solved, at least qualitatively, in both mammals and non mammals. The events, however, are different: sparks –presumably the work of several channels acting in concert– in the frog, and embers –single channels opening– in the rat. Because sparks of

skeletal muscle are understood as a consequence of amplification by CICR of a voltage-initiated channel opening (Klein et al., 1996), this apparent lack of participation of sparks in the functional response of mammalian skeletal muscle is consistent with the conclusion of the whole-cell studies, namely that CICR contributes little or not at all to that response.

## LOCAL CONTROL MODELS IN EC COUPLING: THE COUPLON

The model of dual control of  $\text{Ca}^{2+}$  release proposed by Ríos and Pizarro (1988) was given a more rigorous quantitative treatment by Stern, Pizarro and Ríos (1997). Stern et al. (1999) then extended the model to cardiac EC coupling.

While the model used the idea of a double strip of alternating voltage and  $\text{Ca}^{2+}$ -operated release channels, it added another feature stemming from ultrastructural studies, namely that these strips of channels have a finite length. Contiguous arrays were called EC coupling units by Franzini-Armstrong and Jorgensen (1994). Their length ranges from 0.2 to 0.9  $\mu\text{m}$  (average 0.42  $\mu\text{m}$ ) in the ileofibularis and semitendinosus muscles of the frog (Franzini-Armstrong, Protasi and Ramesh, 1999). The distances between junctional units, 0.1  $\mu\text{m}$  on average, are spanned by non-junctional t-tubule segments that are bare and wavy. Between 10 and 60 release channels should be present on each side of a junctional unit.

Based on such structural data, our approach was to model arrays of a limited length. In order to turn these prescriptions into a concrete model, it was necessary to specify (1) the gating schemes of the  $V$  and  $C$  channels, (2) the permeation kinetics of these channels and (3) the geometry of the junction and conditions of  $\text{Ca}^{2+}$  diffusion and binding therein. The specific assumptions are detailed by Stern et al. (1997). Because the simulations demonstrate that the blockade or inactivation of a single  $C$  channel is sufficient to interrupt  $\text{Ca}^{2+}$ -mediated interaction between channels on both sides of the inactivated one, the groups of channels on one face of one junctional strip turn out to be effectively functionally independent, both from adjacent junctional t-tubule segments, and from the channels on the other face of the junctional segment.

To stress the fundamental nature of the result, we named this functional unit—the set of release channels on one face of one junctional strip, together with its associated voltage sensors and other triadic proteins—a

couplon (Stern, Pizarro and Ríos, 1997; see also Franzini-Armstrong, this issue). There are two couplons per junctional segment of t-tubule.

The result that led to the couplon concept essentially solved the “paradox of control.” Indeed, the fact that a single inactivated channel can stop CICR propagation, together with the natural separation between couplons, makes it possible for an intrinsically self-reinforcing gating scheme to remain at all times under control by the voltage sensors, so that a turn off of the whole set follows rapidly upon movement of the voltage sensors to a deactivating position.

There was a second significant result of the simulations: activations initiated at single voltage-operated channels could propagate to recruit other channels by CICR and produce transients of  $\text{Ca}^{2+}$  release commensurate with observed  $\text{Ca}^{2+}$  sparks.

The couplon model therefore seemed to elegantly account for sparks. The size of the simulated event was consistent with the observations, and both were consistent with the activation of multiple channels (González et al., 2000b; Ríos et al., 1999; Chandler et al., 2003). Also, the simulations resulted in propagation of activation of  $\text{Ca}^{2+}$  channels along the couplon at a velocity of 100-200 microns per millisecond. This was very close to the speed of sparks that were seen moving for short distances in the plane of Z disks under high temporal resolution imaging with a “video-rate” confocal scanner (Brum et al., 2000).

Another contribution from the Schneider laboratory brought these accounts into question, however. Using the video-rate scanner, Lacampagne et al. (1999) showed that the release flux underlying a spark started and ceased abruptly. Abrupt, essentially instantaneous activation and deactivation does not correspond to the gradual sequential recruitment of channels by CICR.

In conclusion, gating simulations assuming  $\text{Ca}^{2+}$ -operated channels result in sparks of adequate size, but gradual activation. Both gradually and abruptly activating sparks have been found in frogs,

and it is unclear what exactly determines these features.

MAMMALIAN SPARKS INVOLVE ARRAYS OF CHANNELS THAT ACTIVATE IN CONCERT

Zhou et al. (2003) explored the differences between sparks of frog and rat. As shown in Figure 6, rat  $Ca^{2+}$  sparks (which as stated above require more artificial conditions to be observed) are spatially wider, even though they tend to be of smaller peak intensity. The widening occurs early in their temporal development, which suggests that the greater spark width corresponds to a spatially wide  $Ca^{2+}$  source, i.e. a large array of  $Ca^{2+}$  release channels.

More interestingly, simulations have not been able to reproduce these events unless the wide source is activated simultaneously. In other words, the spatially wide source of current must reach its value “instantly” (i.e., in less than 1

ms). Because the source needs to be really wide (1 to 3  $\mu\text{m}$ ), the CICR mechanism, which in models accounts for speeds of 100-200  $\mu\text{m/s}$ , appears ill suited to mediate this concerted activation. It may be possible to achieve a much faster activation in CICR simulations by radically changing the model parameters (i.e., reaction rates, diffusion coefficients). However, we believe CICR not to be the mechanism of these fast concerted activations because in the frog it is relatively easy to induce their occurrence, sometimes coexisting with others that propagate at the velocity prescribed by CICR. It seems more likely that two mechanisms coexist, one involving CICR, that results in progression along the couplon at measurable speed (100-200  $\mu\text{m/ms}$ ) and another that results in much faster synchronization of channel opening. Allosteric interactions between RyR channels (Marx et al., 1998) could underlie the second process.

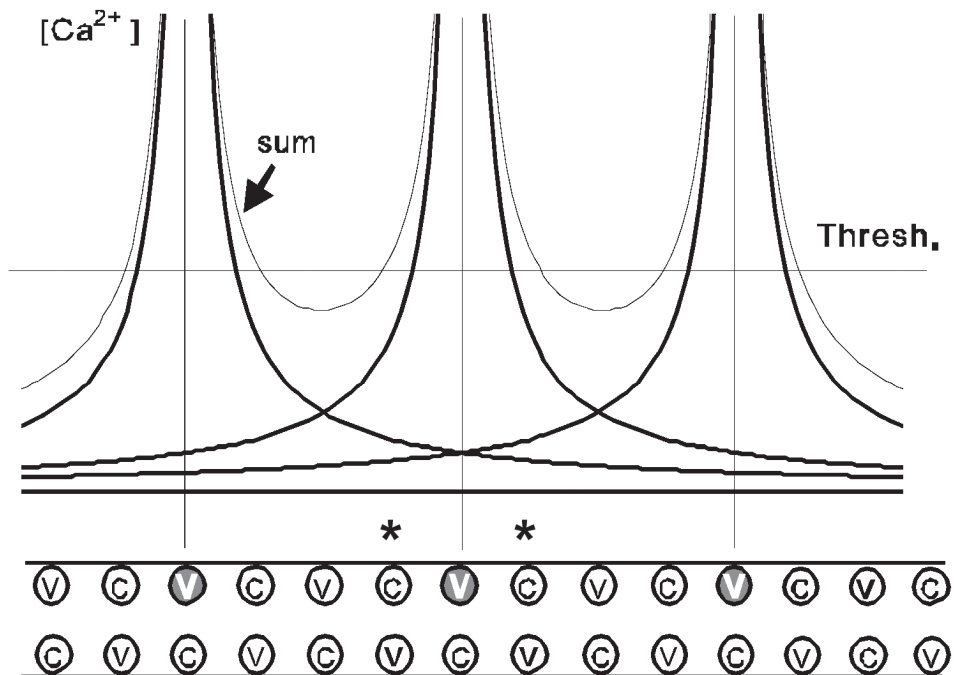


**Figure 4.** Steady  $[Ca^{2+}]$  profiles near open V-operated channels activate  $Ca^{2+}$ -operated channels. At intermediate V, the effect of multiple open V channels is greater than the sum of their effects when opening individually. From Shirokova et al. (1996).

#### THE COUPLON MODEL WAS BUILT ON WRONG ASSUMPTIONS

As we have discussed, the couplon model accounts for some, if not all the characteristics of EC coupling in the frog. This account may be made more complete by assuming the possibility of an allosteric interaction among RyRs, as done in our corresponding model for the cardiac dyadic junction (Stern et al., 1999).

Unfortunately, the model assumed a structure that we now know to be adequate for the rat but not for the frog. This could be a fatal flaw. What the model does best is explain global  $\text{Ca}^{2+}$  release and sparks of the frog. In the rat, we have seen that sparks may not play a major functional role. Worse yet, when they do occur, the activation is much faster than that predicted by the model. These contradictions may be solved with a simple revision to the model, proposed here verbally, in advance of actual simulations.

Two changes must be introduced. First, the idea of dual voltage and  $\text{Ca}^{2+}$ -mediated operation can be reasonably maintained in the frog but not in the rat, as all of the functional evidence indicates little or no operation of CICR in the mammal. Hence, the site of CICR must in all likelihood be the parajunctional RyR3 channels present in the frog but not the rat. These would normally participate in  $\text{Ca}^{2+}$  sparks (the contribution of RyR1 junctional channels to sparks in the frog remaining a question). By contrast, release channels in the rat would be controlled directly by depolarization. Their activation would not spread via CICR.

#### FOR FUTURE STUDIES

Many questions remain. While in the mammal it is easy to imagine a direct, straightforward mechanism of control for the channels that are in direct correspondence with voltage sensors (like the allosteric mechanism proposed by Ríos et al., 1993), the control of the remaining 50% of release channels, those not directly underlying DHPRs, can only be a matter of

speculation. The same question may be posed for the un-paired junctional channels in the frog. Recent 3D reconstructions by Wolf et al. (2003) suggest that the control of the RyRs that are paired with DHPRs and those that are not could have the same mechanism. This is because junctional DHPRs appear to be in a rather peripheral location relative to the underlying RyR tetramer, perhaps in interaction with two neighboring RyRs, so that the same DHPR could be allosterically influencing both  $\text{Ca}^{2+}$  release channels. Allosteric interaction of RyRs among themselves, however, remains the most intriguing alternative. Such interaction could underlie the fast-spreading sparks that can be observed in both species under contrived conditions. Whether such sparks may play a role in mammalian muscle, perhaps at high levels of voltage, is one more question for future studies.

#### ACKNOWLEDGMENTS

We thank C. Franzini-Armstrong and E. Felder for allowing us to use the illustration presented as Figure 1. The work reviewed here would not have been possible without help from many collaborators, including G. Brum, H. Cheng, L. Csernoch, M. Fill, J. García, A. González, B. Launikonis, G. Pizarro, N. Shirokova and M.D. Stern. We were supported by grants from the National Institutes of Health, USA. J. Z. was a Merrick Scholar of Rush University.

#### REFERENCES

- BRUM G, GONZÁLEZ A, RENGIFO J, SHIROKOVA N, RÍOS E (2000) Fast imaging in two dimensions resolves extensive sources of  $\text{Ca}^{2+}$  sparks in frog skeletal muscle. *J Physiol* 528:419-433
- CHANDLER WK, HOLLINGWORTH S, BAYLOR SM (2003) Simulation of calcium sparks in cut skeletal muscle fibers of the frog. *J Gen Physiol* 121: 311-324
- CHENG H, LEDERER WJ, CANNELL MB (1993) Calcium sparks: elementary events underlying excitation-contraction coupling in heart muscle. *Sci* 262:740-744
- CHEUNG HC (2002) Calcium-induced molecular and structural signaling in striated muscle contraction. In: SOLARO RJ, MOSS RL (eds) *Molecular Control Mechanisms in Striated Muscle Contraction*. Norwell, MA: Kluwer Academic Publishers

- CSERNOCH L, ZHOU J, STERN MD, BRUM G, RÍOS E (2004) The elementary events of  $Ca^{2+}$  release elicited by membrane depolarization in mammalian muscle. *J Physiol* 557:43-58
- DELBONO O, STEFANI E (1993) Calcium transients in single mammalian skeletal muscle fibres. *J Physiol* 463:689-707
- FELDER E, FRANZINI-ARMSTRONG C (2002) Type 3 ryanodine receptors of skeletal muscle are segregated in a parajunctional position. *Proc Natl Acad Sci USA* 99:1695-700
- FLUCHER BE, CONTI A, TAKESHIMA H, SORRENTINO V (1999) Type 3 and type 1 ryanodine receptors are localized in triads of the same mammalian skeletal muscle fibers. *J Cell Biol* 146:621-63030
- FRANZINI-ARMSTRONG C, JORGENSEN AO (1994) Structure and development of E-C coupling units in skeletal muscle. *Annu Rev Physiol* 56:509-534
- FRANZINI-ARMSTRONG C, PROTASI F, RAMESH V (1999) Shape, size, and distribution of  $Ca^{2+}$  release units and couplons in skeletal and cardiac muscles. *Biophys J* 77:1528-39
- FRANZINI-ARMSTRONG C (2004) functional implications of RyR-DHPR relationships in skeletal and cardiac muscles. *Biol Res* 37: in this issue
- GARCÍA J, SCHNEIDER MF (1995) Suppression of calcium release by calcium or procaine in voltage clamped rat skeletal muscle fibres. *J Physiol* 485:437-45
- GONZÁLEZ A, KIRSCH WG, SHIROKOVA N, PIZARRO G, STERN MD, RÍOS E (2000a) The spark and its ember. Separately gated local components of  $Ca^{2+}$  release in skeletal muscle. *J Gen Physiol* 115:139-157
- GONZÁLEZ A, KIRSCH WG, SHIROKOVA N, PIZARRO G, BRUM G, PESSAH IN, STERN MD, CHENG H, RÍOS E (2000b) Involvement of multiple intracellular release channels in calcium sparks of skeletal muscle. *Proc Natl Acad Sci USA* 97:4380-4385
- HOLLINGWORTH S, BAYLOR SM, CHANDLER WK (2003) Prolonged, small local  $Ca^{2+}$  releases in frog intact skeletal muscle fibers. *Biophys J* 84:385A
- KIRSCH WG, UTTENWEILER D, FINK RHA (2001) Spark- and ember-like elementary  $Ca^{2+}$  release events in skinned fibres of adult mammalian skeletal muscle. *J Physiol* 537:379-389
- KLEIN MG, CHENG H, SANTANA LF, JIANG YH, LEDERER WJ, SCHNEIDER MF (1996) Two mechanisms of quantized calcium release in skeletal muscle. *Nature* 379:455-458
- KLEIN MG, LACAMPAGNE A, SCHNEIDER MF (1997) Voltage dependence of the pattern and frequency of discrete  $Ca^{2+}$  release events after brief repriming in frog skeletal muscle. *Proc Natl Acad Sci USA* 94:11061-11066
- LACAMPAGNE A, WARD CW, KLEIN MG, SCHNEIDER MF (1999) Time course of individual voltage-activated  $Ca^{2+}$  sparks recorded at ultra-high time resolution in frog skeletal muscle. *J Gen Physiol* 113:187-198
- MARKS AR, TEMPST P, HWANG KS, TAUBMAN MB, INUI M, CHADWICK C, FLEISHER S, NADALGINARD B (1989) Molecular cloning and characterization of the ryanodine receptor/junctional channel complex cDNA from skeletal muscle sarcoplasmic reticulum. *Proc Natl Acad Sci USA* 86:8683-8687
- MARX SO, ONDRIAS K, MARKS AR (1998) Coupled gating between individual skeletal muscle  $Ca^{2+}$  release channels (ryanodine receptors). *Sci* 281:818-821
- MELZER W, RÍOS E, SCHNEIDER MF (1987) A general procedure for determining the rate of calcium release from the sarcoplasmic reticulum in skeletal muscle fibers. *Biophys J* 51: 849-863
- OGAWA Y, KUREBAYASHI N, MURAYAMA T (1999) Ryanodine receptor isoforms in excitation-contraction coupling. *Adv Biophys* 36:27-64
- RÍOS E, PIZARRO G (1988) The voltage sensors and calcium channels of excitation-contraction coupling. *News In Physiol Sci* 3:223-227
- RÍOS E, KARHANEK M, MA J, GONZÁLEZ A (1993) An allosteric model of the molecular interactions of excitation-contraction coupling in skeletal muscle. *J Gen Physiol* 102:449-81
- RÍOS E, STERN MD, GONZÁLEZ A, PIZARRO G, SHIROKOVA N (1999) Calcium release flux underlying  $Ca^{2+}$  sparks of frog skeletal muscle. *J Gen Physiol* 114:31-48
- SCHNEIDER MF, RODNEY GG (2004) peptide and protein modulation of local  $Ca^{2+}$  release events in permeabilized skeletal muscle fibers. *Biol Res* 37: in this issue
- SHIROKOVA N, GARCÍA J, RÍOS E (1996)  $Ca^{2+}$  release from the sarcoplasmic reticulum compared in amphibian and mammalian skeletal muscle. *J Gen Physiol* 107:1-18
- STERN MD, PIZARRO G, RÍOS E (1997) Local control model of excitation-contraction coupling in skeletal muscle. *J Gen Physiol* 110:415-440
- STERN MD, SONG LS, CHENG H, SHAM JS, YANG HT, BOHELER KR, RÍOS E (1999) Local control models of cardiac excitation-contraction coupling A possible role for allosteric interactions between ryanodine receptors. *J Gen Physiol* 113:469-489
- STERN MD (1992) Theory of excitation-contraction coupling in cardiac muscle. *Biophys J* 63:497-517
- SUTKO JL, AIREY JA (1996) Ryanodine receptor  $Ca^{2+}$  release channels: does diversity in form equal diversity in function? *Physiol Reviews* 76: 1027-1071
- SZENTESI P, SZAPPANOS H, SZEGEDI C, GONCZI M, JONA I, CSERI J, ET AL (2004) Altered elementary calcium release events and enhanced calcium release by thymol in rat skeletal muscle. *Biophys J* 86: 1436-1453
- TAKESHIMA H, NISHIMURA S, MATSUMOTO T, ISHIDA H, KANGAWA K, MINAMINO N, MATSUO H, UEDA M, HANAOKA M, HIROSE T NUMA S (1989) Primary structure and expression from complementary DNA of skeletal muscle ryanodine receptor. *Nature* 339:439-445
- TSUGORKA A, RÍOS E, BLATTER L (1995) Imaging elementary events of calcium release in skeletal muscle cells. *Sci* 269:1723-1726
- VOLPE P, SIMON BJ (1991) The bulk of  $Ca^{2+}$  released to the myoplasm is free in the sarcoplasmic reticulum and does not unbind from calsequestrin. *FEBS Lett* 278:274-278
- WOLF M, EBERHART A, GLOSSMANN H, STRIESSNIG J, GRIGORIEFF N (2003) Visualization of the domain structure of an L-type  $Ca^{2+}$  channel using electron cryo-microscopy. *J Mol Biol* 332:171-182
- ZHOU J, BRUM G, GONZÁLEZ A, LAUNIKONIS BS, STERN MD, RÍOS E (2003)  $Ca^{2+}$  sparks and embers of mammalian muscle. Properties of the sources. *J Gen Physiol* 122:95-114